

## METHODS TO EVALUATE THE PERFORMANCE OF SPATIAL SIMULATION MODELS

MONICA G. TURNER<sup>1</sup>, ROBERT COSTANZA<sup>2</sup> and FRED H. SKLAR<sup>3</sup>

<sup>1</sup> *Environmental Sciences Division, Oak Ridge National Laboratory, Oak Ridge, TN 37831-6038 (U.S.A.)*

<sup>2</sup> *Coastal and Environmental Policy Program, Chesapeake Biological Laboratory, University of Maryland, Solomons, MD 20688-0038 (U.S.A.)*

<sup>3</sup> *Baruch Marine Laboratory, University of South Carolina, P.O. Box 1630, Georgetown, SC 29442 (U.S.A.)*

(Accepted 10 April 1989)

### ABSTRACT

Turner, M.G., Costanza, R. and Sklar, F.H., 1989. Methods to evaluate the performance of spatial simulation models. *Ecol. Modelling*, 48: 1–18.

Quantitative methods are necessary to compare spatial patterns and evaluate the performance of spatial simulation models. We present and review several approaches to the analysis and comparison of spatial patterns. The methods are readily applicable to digital data that are in matrix (i.e., grid cell or raster) format, and include: (a) indices of particular aspects of spatial pattern, including fractal dimension, contagion, and interface; (b) spatial predictability; and (c) a variable resolution approach for measuring the degree of fit between two patterns. Because these methods measure different aspects of spatial patterns, they may be differentially suited to particular modeling and analysis objectives. In this paper, we describe the methods, apply each method to a sample data set, then evaluate the information provided and appropriate situations for its use.

### INTRODUCTION

Most ecological simulation models use state variables that vary through time but are spatially aggregated (Costanza and Sklar, 1985). This approach, however, may not be adequate to address current ecological questions at large spatial scales (Risser et al., 1984; DeAngelis and Waterhouse, 1987; Meentemeyer and Box, 1987; Urban et al., 1987). For example, spatial patterning of ecosystems is important in landscape-level models (e.g., Turner, 1987, 1988; Turner et al., 1989), and interactions between spatial elements, such as the flow of energy, materials, and species among component ecosystems, must be incorporated (e.g., Kesner, 1984; Sklar et al., 1985;

Costanza et al., 1986). Comparisons between predicted spatial patterns and actual data are thus required to evaluate spatially explicit models. Established statistical measures of goodness-of-fit can be used for relatively simple comparisons, but new methods may be required to evaluate complex spatio-temporal phenomena.

We present and review several new approaches to the analysis and comparison of spatial patterns. The methods are readily applicable to digital data that are in matrix (i.e., grid cell or raster) format, and include: (a) indices of particular aspects of spatial pattern, including complexity, contagion, interface, and anisotropy; (b) an index of predictability (Colwell, 1974) applied to spatial patterns; and (c) a variable resolution approach for cell by cell comparisons (Costanza, 1989). These methods measure different aspects of spatial patterns, and therefore they may be differentially suited to particular modeling and analysis objectives. In this paper, we describe the methods, apply each method to a sample data set, then evaluate the information and appropriate use of each technique.

## METHODS

### *Indices of spatial pattern*

A variety of indices can be used to quantify overall characteristics of spatial patterns. These indices are useful when statistical aspects of the spatial patterns must be accurately simulated, but the precise location of particular cells is less important.

*Complexity of spatial patterns: Fractal dimension.* Fractal analysis (Mandelbrot, 1977, 1983) was introduced as a method to study spatial patterns that are similar when observed at many scales (i.e., 'self-similar'). Boundaries or shapes can be quantified using fractals, and the fractal dimension can then be used as a measure of the complexity of spatial patterns. This application has been useful in studies of landscape patterns, the spatial patterns resulting from physical, biological and human forces over a geographic area. Fractals have been used to compare simulated and actual landscapes (Gardner et al., 1987; Turner, 1987), to compare the geometry of different landscapes (Krummel et al., 1987; Milne, 1988; O'Neill et al., 1988; Turner and Ruscher, 1988), and to judge the relative benefits to be gained by changing scales in a model or data set (Burrough, 1986). A perimeter to area relationship can be used to calculate the fractal dimension of patch perimeters using grid cell data (Burrough, 1986; Gardner et al., 1987). Using all patches of a single cover type (or all cover types) in a landscape scene, a regression is calculated between  $\log(\text{perimeter}/4)$ , the

length scale used in measuring the perimeter and log (size) of each patch. The fractal dimension of the patch perimeters then equals twice the slope of the regression line. The dimension can range between 1.00 and 2.00, with higher values representing more convoluted boundaries; the expected fractal dimension of a random pattern is 1.5. Calculating the fractal dimension with least-squares is quite reliable, with the  $r^2$  values generally exceeding 0.95.

*Adjacency and contagion: Nearest neighbor probabilities.* Nearest neighbor probabilities,  $q_{i,j}$  – sometimes referred to as Markovian spatial transition probabilities (Lin and Harbaugh, 1984) – represent the probability of cells of land use type  $i$  being adjacent to cells of land use type  $j$ . The  $q_{i,j}$  values are calculated by dividing the number of cells of type  $i$  that are adjacent to type  $j$  by the total number of cells of type  $i$ . A landscape with very large patches of type  $i$  will have a relatively high  $q_{i,i}$ ; however, if the same area of type  $i$  is distributed over many small patches, the  $q_{i,i}$  will be low. Turner (1988) used these probabilities to compare simulated and actual landscape patterns in Georgia.

Probabilities of adjacency are relative easy to calculate with a single pass through a matrix of land cover types. Adjacency information can also be distilled to a single index of the overall contagion (O'Neill et al., 1988) on an  $m \times n$  landscape containing  $s$  cover types using the formula:

$$D_2 = 2s \log s + \sum_{i=1}^m \sum_{j=1}^n q_{i,j} \log q_{i,j} \quad (1)$$

The contagion index,  $D_2$ , measures the extent to which land uses are aggregated or clumped. At high values of  $D_2$ , the summation term deviates from the equiprobable maximum in which all adjacency probabilities are equal, and large, contiguous patches are found in the matrix. At low values of  $D_2$ , the landscape is dissected into many, small patches.

It may also be of interest to compare nearest neighbor probabilities that are calculated both vertically and horizontally such that anisotropism, or directionality, in the spatial pattern can be measured. Directional probabilities are determined by dividing the number of cells of type  $i$  that are horizontally or vertically adjacent to cells of type  $j$  by the total number of cells of type  $i$ . The difference between the horizontal and vertical probabilities of adjacency can indicate directional alignment of spatial components.

*Interface: Edges between components.* The amount of edge between different spatial components may be important for the movement of organisms or materials across boundaries (e.g., Wiens et al., 1985; Turner and Bratton, 1987), and the importance of edge habitat for various species is well known. Thus, it may be important to monitor edges when predicting spatial patterns

and when integrating pattern with function. Edges can be simply calculated by adding both vertical and horizontal edges of cells between land uses and multiplying by the length of the side of a cell.

*Spatial predictability*

Information theoretic concepts were applied to estimating the degree of predictability of periodic phenomena by Colwell (1974). Predictability in this context refers to the reduction in uncertainty about one variable that can be gained from knowledge of another. For example, if the seasonal rainfall pattern in an area is predictable (e.g., there is always a severe dry summer), then knowing the time of year provides information about rainfall (if it's summer, it's probably dry). If there is no relationship between rainfall and season, the rainfall is relatively unpredictable from knowledge of the time of year. Application of these techniques to spatial data measures the reduction in uncertainty about the state of a particular pixel obtained from other knowledge about the pattern. Regularities in spatial data are identified and ranked on a scale from 0 (unpredictable) to 1 (predictable). The result may be interpreted as the degree of departure of the scene from a random

TABLE 1  
Numerical data for the 20×20 base matrix (Fig. 1A)

1	1	3	3	3	1	2	2	2	1	1	3	3	3	3	1	2	2	1	1
1	1	1	1	1	2	1	1	1	1	1	3	3	1	3	1	1	1	2	1
3	3	3	1	3	2	1	2	2	2	1	1	1	1	2	1	1	2	2	
3	3	1	1	1	2	1	2	2	2	1	2	2	2	1	2	2	2	2	
3	3	1	3	1	1	1	1	2	2	2	2	1	1	2	2	2	2	1	
3	3	3	3	1	1	1	1	1	1	1	2	2	2	1	1	1	1	1	
3	1	1	3	3	3	3	1	3	3	3	1	1	2	2	2	1	1	2	
1	1	3	3	3	3	3	3	3	3	3	1	1	2	2	2	2	1	2	
2	2	2	2	2	1	1	1	1	3	3	3	1	1	1	2	2	1	1	
2	2	1	2	2	2	2	2	1	3	3	3	2	2	1	2	2	2	1	
2	2	1	1	2	1	2	1	2	1	1	1	2	2	1	2	2	1	1	
2	1	2	1	2	1	2	2	1	1	1	1	2	2	2	1	2	2	2	
1	1	1	2	2	2	2	2	1	1	1	1	2	2	1	1	2	2	1	
3	3	1	1	2	2	2	2	2	3	3	3	2	2	2	1	1	1	1	
3	3	3	3	1	1	1	3	3	3	1	1	1	1	2	2	2	1	2	
3	3	3	3	2	2	1	3	3	1	2	2	2	1	2	1	1	1	1	
3	1	1	1	2	2	1	1	1	2	2	2	2	1	1	1	1	1	3	
3	1	1	1	2	2	1	1	2	1	1	2	2	1	3	1	1	1	3	
1	1	1	3	2	1	2	2	2	2	1	2	2	1	1	3	3	3	1	
1	1	3	3	1	1	1	2	2	2	2	2	2	2	2	1	1	3	1	

Integers represent different data categories, such as land cover.

(unpredictable) pattern. We develop two measures: (a) spatial adjacency predictability, based on the state of adjacent pixels (similar to the contagion index, but including higher level adjacency information, i.e., the state of adjacent pairs, triplets, quartuples etc.); and (b) spatial address predictability, based on the row or column address of the pixel.

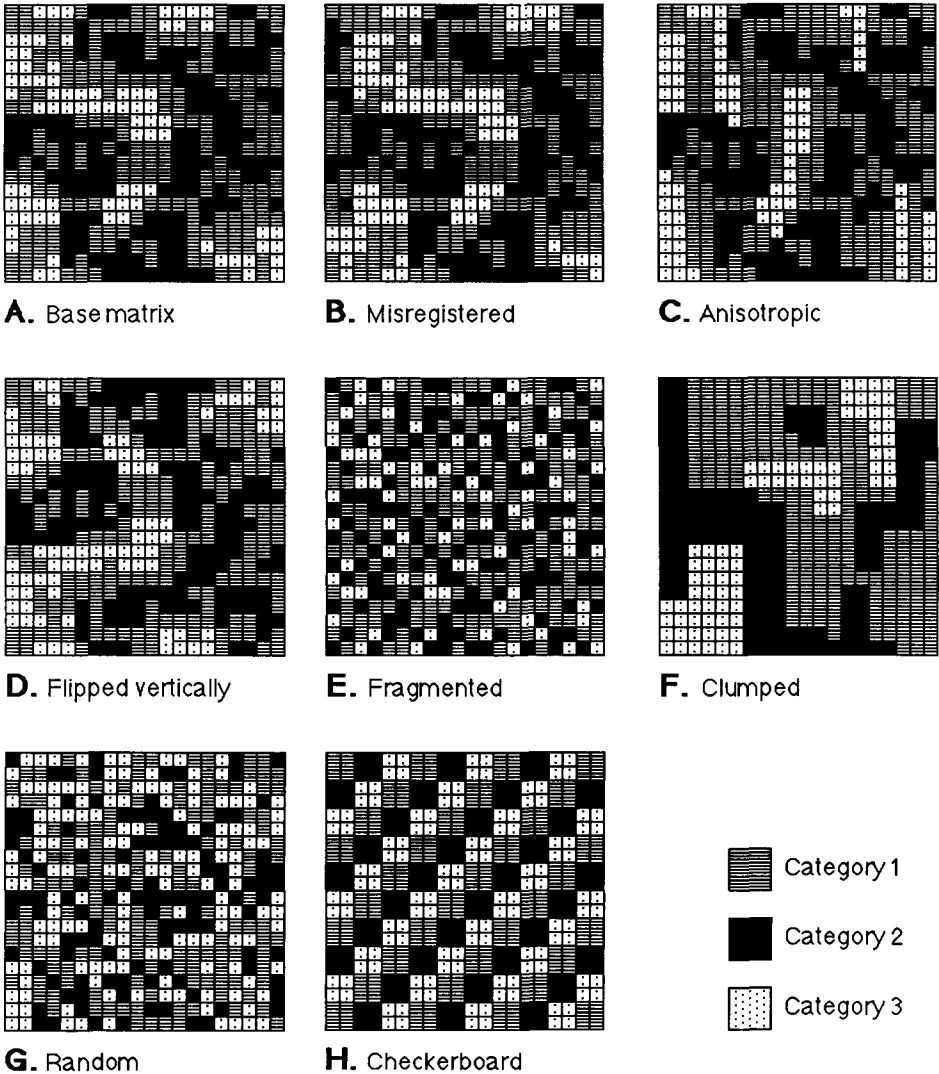


Fig. 1. Test data for demonstrating the methods. All matrices are  $20 \times 20$  arrays with three categories (e.g., land cover, vegetation, ec.) each. Matrices A through G have the same proportions of each category (category 1 = 0.45; category 2 = 0.35; category 3 = 0.20). Matrix H has an approximately equiprobable distribution of the three categories.

TABLE 2

First-order contingency table used to calculate spatial predictability for the  $20 \times 20$  matrix in Table 1

Category	Category			Totals $Y_i$
	1	2	3	
1	187	104	55	346
2	102	161	8	271
3	52	2	89	143
Totals ( $X_j$ )	341	267	152	760 <sup>a</sup>

Entries ( $N_{i,j}$ ) are the frequency that the column category is followed by the row category, either horizontally or vertically (e.g., category 1 is followed by category 2, 102 times; category 2 is followed by category 1, 104 times). First-order predictability ( $P_1$ ) = 0.222.

<sup>a</sup> Note that for an  $m \times m$  matrix, the total is equal to  $2[m \times (m - 1)]$  which is  $2(20 - 19)$  in this example.

To estimate spatial adjacency predictability, a contingency matrix is developed with rows corresponding to the states of the pixels, and columns corresponding to groups of  $n$  pixels. For example, using numerical data of the scene in Fig. 1A (Table 1), first-order ( $n = 1$ ; Table 2) and second-order ( $n = 2$ ; Table 3) contingency matrices were developed. The rows represent the three cover types, and the matrix entries are the number of times each row category occurred adjacent to the column category (or category pair [as in Table 2], triplet, etc. in higher-order analyses) represented by each column. The second-order contingency matrix (Table 3) incorporates greater detail than the first, tabulating the number of times that an ordered pair of categories is adjacent to another category (e.g., how frequently are two forest pixels followed by a grassland pixel). Higher-order matrices continue to incorporate more information, representing the frequency that an ordered group of  $n$  pixels is adjacent to a particular category.

TABLE 3

Second-order contingency table for the  $20 \times 20$  matrix in Table 1

Category	Category pairs									Totals $Y_i$
	11	12	13	21	22	23	31	32	33	
1	86	29	12	58	66	0	31	3	36	321
2	57	68	3	30	85	0	13	5	5	266
3	33	0	34	10	2	2	9	0	43	133
Totals ( $X_j$ )	176	97	49	98	153	2	53	8	84	720 <sup>a</sup>

Entries ( $N_{i,j}$ ) are the frequency that the column category (ordered pairs) is followed by the row category (either horizontally or vertically). Second-order predictability ( $P_2$ ) = 0.228.

<sup>a</sup> Note that for an  $m \times m$  matrix, the total is equal to  $2[m \times (m - 2)]$  which is  $2(20 - 18)$  in this example.

To estimate predictability based on the location of the pixel in the land use matrix (address predictability), the contingency matrix is developed with rows corresponding to the states of the pixels. The columns in the contingency matrix represent the row or column location of a pixel in the land use matrix (e.g., rows 1 through 20). Matrix entries represent the number of occurrences of each state in each row or column. Address predictability may be sensitive to banded patterns in the data.

Following Colwell (1974) we define  $N_{ij}$  as the elements in the contingency matrix of size  $s$  by  $t$ ,  $X_j$  as the column totals,  $Y_i$  as the row totals, and  $Z$  as the grand total, or:

$$X_j = \sum_{i=1}^s N_{ij} \quad (2)$$

$$Y_i = \sum_{j=1}^t N_{ij} \quad (3)$$

$$Z = \sum_{i=1}^s \sum_{j=1}^t N_{ij} \quad (4)$$

The uncertainty with respect to  $X$  is:

$$H(X) = - \sum_{j=1}^t \frac{X_j}{Z} \log \frac{X_j}{Z} \quad (5)$$

and the uncertainty with respect to  $Y$  is:

$$H(Y) = - \sum_{i=1}^s \frac{Y_i}{Z} \log \frac{Y_i}{Z} \quad (6)$$

and the uncertainty with respect to the interaction of  $X$  and  $Y$  is:

$$H(XY) = - \sum_i \sum_j \frac{N_{ij}}{Z} \log \frac{N_{ij}}{Z} \quad (7)$$

Note that the first-order contingency matrix is related to the matrix of nearest neighbor probabilities ( $Q$ ) by the relationship  $N_{ij}/X_j = q_{ij}$ . The conditional uncertainty of  $X$  given  $Y$  is:

$$H_x(Y) = H(XY) - H(X) \quad (8)$$

Finally, a measure of predictability ( $P$ ) with the range (0, 1) can be defined as:

$$P = 1 - \frac{H_x(Y)}{\log s} = 1 - \frac{H(XY) - H(X)}{\log s} \quad (9)$$

Predictability will be minimal when all the elements in the contingency

matrix ( $N_{ij}$ ) are equiprobable (i.e., when all entries are the same) and will be maximized when only one entry in each column is non-zero. Most spatial data will fall between these extremes. For example, the contingency matrix in Table 2 has a predictability of 0.222 indicating that if the state of a given pixel is known, the uncertainty about the state of the following pixel (either horizontally or vertically) is reduced by 22.2%. Highly clumped patterns will have a high adjacency predictability. First-order spatial predictability ( $P_1$ ) and the contagion index ( $D_2$ ) yield similar, but not identical, information. However,  $P$  is scaled on the range (0, 1) whereas  $D_2$  is not.

### *Multiple resolution goodness-of-fit*

A cell by cell comparison between a model's predicted spatial patterns and the actual patterns is necessary if the location of different habitats relative to their actual locations is important. However, a comparison done only at a fine resolution may not adequately evaluate the prediction. A standard fit procedure can be applied at a number of spatial resolutions, and the change in fit with resolution of the sampling window may be a better tool for interpreting the patterns predicted by a model (Costanza, 1989). We use an algorithm for this purpose that gradually decreases the resolution of comparison by increasing the size of the sampling window used to calculate the fit. For a sampling window size of one cell (the cell by cell comparison), the fit is the proportion of cells that are correctly matched, regardless of their spatial arrangement. For example, if a particular  $2 \times 2$  window had two cells of forest and two of marsh in both scenes, the fit would be 100% regardless of how the cells were arranged within the windows. If one sampling window had one forest and three marsh, while the other had two of each category, the fit would be 75% (three out of four were correct). The sampling window is moved through the scene one cell at a time until the entire image is covered. The average fit over all sampling windows of a particular size is then calculated, representing the overall fit at that resolution.

The formula for the fit at a particular sampling window size ( $F_w$ ) is:

$$F_w = \frac{\sum_{s=1}^{t_w} \left[ 1 - \frac{\sum_{i=1}^p |a_{1i} - a_{2i}|}{2w^2} \right] s}{t_w} \quad (11)$$

where  $F_w$  is the fit for sampling window size  $w$ ,  $w$  the dimension of one side of the (square) sampling window,  $a_{ki}$  the number of cells of category  $i$  in scene  $k$  in the sampling window,  $p$  the number of different categories (e.g.,

habitat types) in the sampling windows,  $s$  the sampling window of dimension  $w$  by  $w$  which slides through the scene one cell at a time, and  $t_w$  the total number of sampling windows in the scene for window size  $w$ .

If two scenes were identical, a plot of  $F_w$  against  $w$  would yield a straight line at  $F_w = 1.00$ . If the scenes had the same proportions of cover types but the spatial patterns were very different, the line would increase gradually until the window size was the same as the study area, at which point it would reach  $F_w = 1.00$ . If there were slight differences in the two patterns, the curve would increase rapidly at first then asymptotically approach  $F_w = 1.0$ , indicating that the patterns were relatively well-matched. If two randomly generated scenes with  $s$  cover types were compared, the expected fit would start at  $1/s$  and rapidly increase to 1 as the expanding sampling window encompassed the statistical similarity between the two scenes.

An overall index of fit can be calculated as a weighted average of the fits at different window sizes. By selecting the value of a constant,  $k$ , in the following formula, differential weight can be assigned to particular window sizes:

$$F_t = \frac{\sum_{w=1}^n F_w e^{-k(w-1)}}{\sum_{w=1}^n e^{-k(w-1)}} \quad (12)$$

where  $F_t$  is weighted average of the fits over all window sizes,  $F_w$  the fit for sampling windows of linear dimension  $w$ ,  $k$  a constant, and  $w$  linear dimension of a sampling window. When  $k = 0$ , all window sizes are given the same weight. When  $k = 1$ , only the smaller window sizes are important. The value of  $k$  can be adjusted depending on the model objectives and the quality of the data.

## DATA

Sample  $20 \times 20$  matrices (Fig. 1) were used to compare the methods described above. Matrices A through G contain three cover types (considered to represent any kind of categorical data) in the same proportions ( $p_1 = 0.45$ ;  $p_2 = 0.35$ ;  $p_3 = 0.20$ ). However, the spatial arrangements of the cover types vary. Matrix A (Fig. 1A) is the base case, which is then altered (Fig. 1) by: misregistration (B); by creating anisotropy in one cover type (C); by flipping the matrix vertically (D); by creating a fragmented pattern (E); and by creating a highly clumped pattern (F). Matrix G is a random pattern that maintains the same category proportions as the other matrices (Fig. 1G). Matrix H is a checkerboard (Fig. 1H) with the three categories in equal proportions ( $p_1 = p_2 = p_3 = 0.33$ ).

## RESULTS

*Indices of spatial patterns*

The fragmented and random matrices (Fig. 1E and G) exhibit the most complex spatial patterns as measured by the fractal dimension (Table 4). The anisotropic matrix (Fig. 1C) has a relatively simple overall pattern, reflected by a fractal dimension of 1.469, although the clumped pattern should give a lower result if there was a sufficient number of patches to use for the calculations. The checkerboard matrix (Fig. 1H) has the most simple patch shapes (all squares), whose perimeters have a fractal dimension of 1.0, by definition. The fractal dimensions in matrices A, B and D show little

TABLE 4

Spatial indicators for sample matrices (Fig. 1) having the same fraction of the matrix occupied by different cover types ( $p_1 = 0.45$ ;  $p_2 = 0.35$ ;  $p_3 = 0.20$ )

Measure	Matrix							
	A Original	B Misreg- istered	C Aniso- tropic	D Flipped	E Frag- mented	F Clumped	G Random	H Checker- board
<i>Fractal dimension</i>								
Overall	1.506	1.513	1.469	1.506	1.629	– <sup>a</sup>	1.622	1.000 <sup>b</sup>
Cover type 1	1.565	1.577	1.542	1.565	1.678	– <sup>a</sup>	1.712	1.000 <sup>b</sup>
Cover type 2	1.467	1.481	1.453	1.467	1.506	– <sup>a</sup>	1.559	1.000 <sup>b</sup>
Cover type 3	1.432	1.433	1.199	1.432	1.450	– <sup>a</sup>	1.504	1.000 <sup>b</sup>
<i>Probabilities of adjacency</i>								
$q_{11}$ Horizontal	0.586	0.565	0.547	0.586	0.433	0.847	0.413	0.531
$q_{11}$ Vertical	0.512	0.512	0.659	0.512	0.310	0.831	0.419	0.531
$q_{22}$ Horizontal	0.615	0.597	0.615	0.615	0.231	0.715	0.417	0.524
$q_{22}$ Vertical	0.591	0.591	0.583	0.578	0.191	0.884	0.377	0.524
$q_{33}$ Horizontal	0.618	0.628	0.387	0.618	0.093	0.750	0.203	0.524
$q_{33}$ Vertical	0.553	0.553	0.813	0.575	0.107	0.851	0.128	0.524
<i>Contagion (<math>D_2</math>)</i>								
Horizontal	4.112	4.016	3.877	4.112	3.583	4.641	3.422	4.516
Vertical	4.045	4.045	4.389	4.067	3.640	5.141	3.468	4.516
Average	4.078	4.035	4.133	4.089	3.612	4.891	3.445	4.516
<i>Edges</i>								
1 and 2	206	205	192	206	291	80	225	120
1 and 3	107	110	85	107	142	36	125	120
2 and 3	10	13	26	10	128	24	139	120
Total	323	328	303	323	561	140	489	360

<sup>a</sup> insufficient number of patches for reliable regression.

<sup>b</sup> cannot be calculated by regression; all patches are perfect squares and their perimeters are straight lines.

difference, reflecting the similarity in their spatial patterns. The decreased complexity in cover type 3 in the anisotropic matrix is measured by a low fractal dimension of 1.199.

The probabilities of adjacency (Table 4) appear more sensitive to fine differences in pattern than the fractal dimension. All horizontal  $q_{i,i}$ 's exceed the vertical  $q_{i,i}$ 's in matrix A, indicating a slight horizontal orientation. When A is misregistered by two columns, as in matrix B, the horizontal  $q_{i,i}$ 's change slightly while the vertical  $q_{i,i}$ 's remain the same. Thus, the probabilities are sensitive to slight changes in spatial adjacencies. The anisotropy of a spatial component is also readily apparent in differences between horizontal and vertical adjacencies. For example, the vertical orientation of cover type 3 in matrix C (Fig. 1C) is reflected in the difference between  $q_{3,3}$  vertical (0.813) and  $q_{3,3}$  horizontal (0.387) (Table 4). In contrast, when spatial patterns are very fragmented (matrix E) or clumped (matrix F), the  $q_{i,i}$ 's are low or high, respectively, but show little difference between the horizontal and vertical directions. The isotropic pattern (matrix H) exhibits no difference in horizontal and vertical adjacencies.

The contagion index differentiates the fragmented ( $D_2 = 3.612$ ) and clumped ( $D_2 = 4.891$ ) matrices (Table 4), suggesting that  $D_2$  may be an adequate indicator of broad-scale pattern. However,  $D_2$  is not sensitive to the vertical inversion (Fig. 1D) or to misregistration (Fig. 1B). The checkerboard pattern also has a relatively high contagion value (4.516) indicating a clumped pattern. Although contagion does not necessarily reflect directionality, anisotropy can be identified in differences between vertical and horizontal contagion values (4.389 and 3.877, respectively, in matrix C). However, the cause of directionality (i.e., which components are anisotropic) cannot be determined using  $D_2$  alone.

The amount of edge in the matrices is not sensitive to the precise spatial patterns (Table 4). The edges present in matrices A, B, C and D are quite similar although the locations of the patches vary. Edges values are inversely related to the contagion in the matrix, such that patterns with low contagion have many edges (matrices E and G) and patterns with high contagion have few edges (matrix F).

### *Spatial predictability*

Matrices A through D are similar in their adjacency predictability (Table 5); all have a  $P_1$  of approximately 0.2. This is not surprising because their spatial patterns are statistically similar (Table 4). The adjacency predictability clearly differentiates matrices A–D from the clumped matrix ( $P_1 \approx 0.47$ ) and the fragmented and random matrices ( $P_1 \approx 0.07$  and 0.04, respectively). The predictabilities measured in the random and fragmented matrices ap-

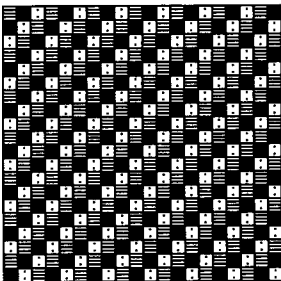
TABLE 5

Summary of predictability measures applied to the test data

Matrix	Matrix							
	A	Misregistered B	Anisotropic C	Flipped vertically D	Frag-mented E	Clumped F	Random G	Checkerboard H
<i>Spatial adjacency predictability</i>								
$P_1$	0.2219	0.2042	0.2062	0.2178	0.0751	0.4674	0.0376	0.3700
$P_2$	0.2283	0.2133	0.2103	0.2222	0.0826	0.4799	0.0447	1.0000
$P_3$	0.2617	0.2692	0.2601	0.2589	0.1102	0.5266	0.0739	1.0000
$P_4$	0.2999	0.3024	0.3093	0.3030	0.1923	0.5548	0.1586	1.0000
<i>Spatial address predictability</i>								
$P_x$	0.120	0.120	0.222	0.120	0.067	0.221	0.066	0.009
$P_y$	0.129	0.129	0.097	0.129	0.081	0.144	0.083	0.009
$P_{\text{avg}}$	0.124	0.124	0.159	0.124	0.074	0.182	0.074	0.009

$P_1$  through  $P_4$  refer to the predictability of the state of a pixel given the states of groups of one, two, three, and four adjacent pixels.  $P_x$  and  $P_y$  refer to the predictability of a pixel given only its row ( $x$ ) or column ( $y$ ).  $P_{\text{avg}}$  is the average of  $P_x$  and  $P_y$ .

proach, but do not reach, zero. This is because the proportions are not equiprobable and our examples are finite, relatively small matrices. Using address predictability (Table 5), the anisotropic matrix is more predictable if the row address is known than if the column address is known ( $P_x = 0.222$

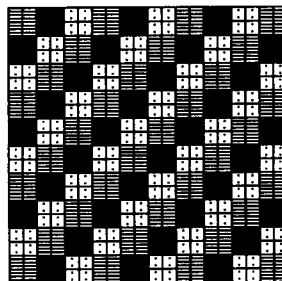
**A.** Checkerboard 1

$$P_1 = 1.00$$

$$P_2 = 1.00$$

$$P_3 = 1.00$$

$$P_4 = 1.00$$

**B.** Checkerboard 2

$$P_1 = 0.37$$

$$P_2 = 1.00$$

$$P_3 = 1.00$$

$$P_4 = 1.00$$

Fig. 2. Repeating checkerboard patterns at different base scales. Both patterns are predictable, but this is not apparent in B until the second order predictability analysis is done because the pattern is composed of  $2 \times 2$  blocks of pixels.

and  $P_Y = 0.097$ ), reflecting the vertical bands that were introduced into matrix C. The checkerboard matrix is least predictable from knowledge of the row or column address of a cell ( $P_x = P_Y = 0.009$ ), because each row and column are statistically identical.

There are no large breaks or periodicities in the patterns in matrices A through F, and higher order adjacency predictabilities ( $P_1-P_4$ ) yield little additional information about these patterns (Table 5). However, the multi-level analysis does elicit significant additional information in certain cases. In the checkerboard matrix, second-order spatial predictability is 1.00, indicating complete predictability at that scale. Thus, spatial predictability can identify the spatial scales of periodicities in a pattern. For example, the scale of the checkerboard pattern is one pixel in Fig. 2A, whereas the pattern repeats every two pixels in Fig. 2B. Spatial predictability ( $P_1$  through  $P_4$ ) is 1.0 for the pattern in Fig. 2A, as the periodicity is apparent even in the first-order analysis. The pattern in Fig. 2B has low predictability with a first-order analysis ( $P_1 = 0.370$ ) because the periodicity is not apparent at this level, but the second order analysis indicates complete predictability. Therefore, the most appropriate use of the higher-order predictabilities may be to identify patterns that show periodicity at different spatial scales.

*Multiple resolution fitting*

Results of the multiple resolution fitting analyses (Table 6, Fig. 3) indicate that the base matrix is most similar to the anisotropic matrix (at  $k = 0.1$ ,  $F_i = 0.914$ ). The positions of pixels of category 2 were retained

TABLE 6

Goodness-of-fit between the original matrix (A) and other matrices using (1) the multiple resolution fit procedure and differential weighting of the windows and (2) cross predictability, which is the predictability of a pixel on one map given its corresponding state on another map

Comparison	Weighted average of goodness-of-fit ( $F_i$ )				Cross predictability $P_c$
	$k = 0.0$	$k = 0.01$	$k = 0.1$	$k = 1.00$	
A × B: Misregistered	0.821	0.815	0.764	0.541	0.1016
A × C: Anisotropic	0.930	0.928	0.914	0.856	0.6475
A × D: Flipped vertically	0.793	0.787	0.736	0.500	0.0657
A × E: Fragmented	0.856	0.852	0.821	0.702	0.2363
A × F: Clumped	0.709	0.702	0.649	0.460	0.0544
A × G: Random	0.768	0.761	0.706	0.450	0.0465
G × G: Random × Random	0.801	0.800	0.753	0.502	0.0757
E × G: Fragmented × Random	0.829	0.823	0.775	0.495	0.0406

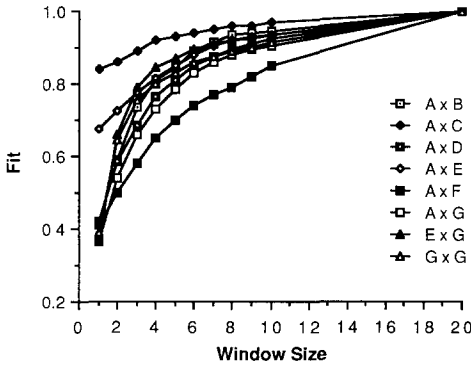


Fig. 3. Fit versus window size for various pairs of the matrices in Fig. 1 using the multiple resolution fitting method. For example,  $A \times B$  is the comparison of the base matrix (A) with the misregistered matrix (B).

when anisotropy was introduced, and only a small fraction of the other two categories was rearranged. Thus, a relatively high cell by cell agreement is observed between the anisotropic and base matrices.

The fragmented pattern exhibits the next best fit (at  $k = 0.1$ ,  $F_t = 0.821$ ) with the base matrix. This seems counter-intuitive, because the fragmented and random patterns are similar (Tables 4 and 5). However, the fragmented pattern was created from the base matrix by arbitrarily rearranging some of the pixels in Fig. 1A and not by randomly creating a new pattern. Therefore, more pixels in the fragmented pattern correspond to pixels in the base matrix ( $\approx 68\%$ ) than expected at random ( $\approx 33\%$ ), even though the fragmented and random patterns appear similar.

The base matrix does not fit well with the clumped or random patterns, as might be expected. However, the misregistered and vertically flipped matrices also do not fit well with the base matrix, although their patterns are identical except for slight misregistration. This result indicates a limitation of the multiple resolution fitting procedure and suggests the need to handle misregistration problems separately (Costanza, 1989). If registration between patterns is questionable, a cross-correlation analysis could be used to determine the point of maximum registration. After the maps have been registered, the multiple resolution fitting procedure should produce more reasonable results.

Cross predictability ( $P_c$ ) can be calculated for pairs of maps to determine the predictability of the state of pixels on one map given their corresponding state on another map. This is another goodness-of-fit test and the results for our example maps are included in Table 6. This index of fit correlates well with the multiple resolution test ( $r^2 = 0.918$  for  $k = 1.0$ ) but yields a different perspective and range of values. Values for this test range from

approximately 0.04 for comparisons with random maps to 0.66 for the base map compared with the anisotropic case. This indicates that knowledge of the category of a pixel on the base map removes 66% of the uncertainty about its state on the anisotropic map, but this knowledge removes only 4.6% of the uncertainty about its state on a random map.

DISCUSSION

What information is provided by each of these methods? And what is the relative cost to calculate each one? A brief summary is presented in Table 7. The indices of spatial pattern (fractal dimension, nearest neighbors probabilities, contagion, edges, spatial predictability) give statistical measures of whether certain aspects of the pattern are comparable, but do not indicate whether the cell by cell pattern is exactly (or approximately) matched. This may be adequate when one wishes to predict overall behavior of a system, or

TABLE 7  
Summary of methods for quantifying and comparing spatial patterns

Measure	Characteristic	Computation	Use
Fractal dimension	complexity of spatial pattern	identify size and area of each path (time and memory intensive; can be unreliable for small patches)	broad-scale measure of pattern; may reflect scale of processes creating pattern
Nearest neighbor probabilities	adjacency and anisotropy	single pass through the matrix (fast, even for large matrices)	fine-scale measure of pattern and directionality
Contagion index	fragmentation or clumping	uses the probabilities of adjacency (fast)	overall measure; can also identify anisotropy
Edges	edge between components	single pass through the matrix (fast)	when exact amount of interface is important
Spatial predictability	departure from random; periodicity at different scales	uses $n$ th order probabilities of adjacency	departure from random on a (0, 1) scale; scale-dependent patterns
Multiple resolution fitting	correspondence to actual locations	calculates goodness-of-fit with decreasing resolution	pattern matching when accurate spatial locations are required between matrices

when these pattern aspects are otherwise important. The fractal dimension measures pattern complexity, providing information about patch shape, but does not address the adjacency of different cover types. The fractal has also been hypothesized to reflect the scale of the factors causing the pattern (Krummel et al., 1987). Nearest neighbor probabilities provide a fine-scale measure of adjacency patterns and the directionality of individual cover types. Nearest neighbor probabilities also reflect the degree of fragmentation in the landscape and, indirectly, the complexity of patch boundaries. The contagion index measures the dissection or clumping in the spatial pattern, but does not identify the factors causing the pattern. Edge calculations provide the amount of interface between different categories, but they are not sensitive to specific spatial arrangements. Spatial predictability measures the degree of departure from a random pattern and identifies periodicities in spatial patterns at different scales. First-order spatial adjacency predictability and the contagion index are highly correlated ( $r^2 = 0.99$ ), but predictability may be easier to interpret because it is scaled on the range (0, 1).

The multiple resolution fitting method compares spatial data on a cell by cell basis, but it is not sensitive to qualitative differences between spatial patterns. It may be particularly useful when the patterns are only slightly different, and if the patterns are properly registered. An advantage of the multiple resolution measure is its sensitivity to a periodic patterns or clusters and its lack of sensitivity to pattern complexity. The method can be used if simulating the actual location of categorical data is important. However, because of its insensitivity to qualitative aspects of the pattern (e.g., clumped versus dissected, complex versus simple), another indicator of spatial pattern might be used to supplement multiple resolution fitting if these aspects of the pattern are important.

Additional characteristics must be considered when selecting a method for comparing simulated and actual spatial patterns. The matrices should be of the same dimensions, because matrix size has been shown to affect the number, size, and shape (as measured by the fractal dimension) of clusters (Gardner et al., 1987). The grid cells should also be of the same resolution, or grain size, as pattern measures have been shown to vary with scale (Turner et al., in press). Data sets should contain the same number of data categories if indices based on information theory (e.g., contagion, spatial predictability) are to be used. Matrices must also be properly registered to obtain valid results from the multiple resolution fitting method. Computational considerations may also be important. For example, calculating fractal dimensions can require considerable computer memory and time with large matrices, because each patch in a matrix must be located and its area and perimeter recorded. In contrast, adjacency, contagion, edges and predictability can all be calculated on a single pass through the matrix.

The issue of significant (both statistically and ecologically) changes or differences in spatial patterns remains an important research topic. Statistically significant differences in spatial data can be determined by a variety of techniques, and S. Turner et al. (in press) have recently reviewed many of the available methods. However, slight differences or changes in spatial patterns may result in substantial alterations in ecological processes, but this aspect is not well known. The existence of thresholds in spatial patterns (Gardner et al., 1987; Turner et al., 1989) may be quite important in governing whether or not a change in pattern results in qualitatively different system behavior. It also remains necessary to determine the ecological significance of differences in broad-scale pattern indices (e.g., contagion, fractal dimension, predictability). Additional research is required to elucidate these topics.

The methods we have presented are useful for examining the goodness-of-fit between spatial simulations and data. The selection of appropriate methods will depend on specific modeling objectives and on the attributes of the data. Additional research in pattern analysis and comparison should improve the evaluation of landscape models, and therefore enhance our ability to simulate broad-scale phenomena, characterize spatial patterns, and ultimately manage natural resources at the landscape level.

#### ACKNOWLEDGEMENTS

We thank Robert H. Gardner and Robert V. O'Neill for their critical comments on the manuscript. This research was funded, in part, by the Ecological Research Division, Office of Health and Environmental Research, U.S. Department of Energy, under Contract No. DE-AC05-84OR21400 with Martin Marietta Energy Systems, Inc., and by an Alexander Hollaender Distinguished Postdoctoral Fellowship, administered by Oak Ridge Associated Universities, to M.G. Turner. Funding for R. Costanza and F.H. Sklar was provided, in part, by Cooperative Agreement No. 14-16-0009-84-921 between the U.S. Fish and Wildlife Service and the Coastal Ecology Institute, Center for Wetland Resources, Louisiana State University.

This is Publication No. 3290 of the Environmental Sciences Division, Oak Ridge National Laboratory.

#### REFERENCES

- Burrough, P.A., 1986. Principles of Geographic Information Systems for Land Resources Assessment. Clarendon, Oxford, 194 pp.
- Colwell, R.K., 1974. Predictability, constancy, and contingency of periodic phenomena. *Ecology*, 55: 1148–1153.
- Costanza, R., 1989. Model goodness of fit: a multiple resolution procedure. *Ecol. Modelling*, 47: 47: 199–215.

- Costanza, R. and Sklar, F.H., 1985. Articulation, accuracy, and effectiveness of mathematical models: a review of freshwater wetland applications. *Ecol. Modelling*, 27: 45–68.
- Costanza, R., Sklar, F.H. and Day, J.W., Jr., 1986. Modeling spatial and temporal succession in the Atchafalaya/Terrebonne marsh/estuarine complex in South Louisiana. In: D.A. Wolfe (Editor), *Estuarine Variability*. Academic Press, New York, pp. 387–404.
- DeAngelis, D.L. and Waterhouse, J.C., 1987. Equilibrium and nonequilibrium concepts in ecological models. *Ecol. Monogr.*, 57: 1–21.
- Gardner, R.H., Milne, B.T., Turner, M.G. and O'Neill, R.V., 1987. Neutral models for the analysis of broad-scale landscape pattern. *Landscape Ecol.*, 1: 19–28.
- Kesner, B.T., 1984. The geography of nitrogen in an agricultural watershed: a technique for the spatial accounting of nutrient dynamics. Masters thesis, University of Georgia, Athens, GA.
- Krummel, J.R., Gardner, R.H., Sugihara, G. and O'Neill, R.V., 1987. Landscape patterns in a disturbed environment. *Oikos*, 48: 321–324.
- Lin, C. and Harbaugh, J.W., 1984. *Graphic Display of Two- and Three-Dimensional Markov Computer Models in Geology*. Van Nostrand Reinhold, New York, 192 pp.
- Mandelbrot, B.B., 1977. *Fractals. Form, Chance and Dimension*. Freeman, San Francisco, CA.
- Mandelbrot, B.B., 1983. *The Fractal Geometry of Nature*. Freeman, San Francisco, CA, 460 pp.
- Meentemeyer, V. and Box, E.O., 1987. Scale effects in landscape studies. In: M.G. Turner (Editor), *Landscape Heterogeneity and Disturbance*. Springer, New York, pp. 15–34.
- Milne, B.T., 1988. Measuring the fractal dimension of landscape. *Appl. Math. Comput.*, 27: 67–79.
- O'Neill, R.V., Krummel, J.R., Gardner, R.H., Sugihara, G., Jackson, B., DeAngelis, D.L., Milne, B.T., Turner, M.G., Zymunt, B., Christensen, S., Dale, V.H. and Graham, R.L., 1988. Indices of landscape pattern. *Landscape Ecol.*, 1: 153–162.
- Risser, P.G., Karr, J.R., and Forman, R.T.T., 1984. *Landscape ecology: directions and approaches*. Spec. Publ. 2, Illinois Natural History Survey, Champaign, IL, 18 pp.
- Sklar, F.H., Costanza, R. and Day, J.W., Jr., 1985. Dynamic spatial simulation modeling of coastal wetland habitat succession. *Ecol. Modelling*, 29: 261–281.
- Turner, M.G., 1987. Spatial simulation of landscape changes in Georgia: a comparison of 3 transition models. *Landscape Ecol.* 1: 29–36.
- Turner, M.G., 1988. A spatial simulation model of land use changes in Georgia. *Appl. Math. Comput.*, 27: 39–51.
- Turner, M.G. and Bratton, S.P., 1987. Fire, grazing and the landscape heterogeneity of a Georgia barrier island. In: M.G. Turner (Editor), *Landscape Heterogeneity and Disturbance*. Springer, New York, pp. 85–101.
- Turner, M.G. and Ruscher, C.L., 1988. Changes in the spatial patterns of land use in Georgia. *Landscape Ecol.*, 1: 241–251.
- Turner, M.G., Gardner, R.H., Dale, V.H. and O'Neill, R.V., 1989. Predicting the spread of disturbance across heterogeneous landscapes. *Oikos*, 55: 121–129.
- Turner, M.G., O'Neill, R.V., Gardner, R.H. and Milne, B.T., in press. Effects of changing spatial scale on the analysis of landscape pattern. *Landscape Ecol.*
- Turner, S.J., O'Neill, R.V., Conley, W., Conley, M.R. and Humphries, H.C., in press. Pattern and scale: statistics for landscape ecology. In: M.G. Turner and R.H. Gardner (Editors), *Quantitative Methods in Landscape Ecology*. Springer, New York.
- Urban, D.L., O'Neill, R.V. and Shugart, H.H., 1987. Landscape ecology, a hierarchical perspective. *BioScience*, 37: 119–127.
- Wiens, J.A., Crawford, C.S. and Gosz, J.R., 1985. Boundary dynamics: a conceptual framework for studying landscape ecosystems. *Oikos*, 45: 421–427.